Quantum Mechanical Limitations to Spin Diffusion in the Unitary Fermi Gas

Tilman Enss

Physik Department, Technische Universität München, D-85747 Garching, Germany

Rudolf Haussmann

Fachbereich Physik, Universität Konstanz, D-78457 Konstanz, Germany
(Received 13 July 2012; published 9 November 2012)

We compute spin transport in the unitary Fermi gas using the strong-coupling Luttinger-Ward theory. In the quantum degenerate regime the spin diffusivity attains a minimum value of $D_s \simeq 1.3\hbar/m$ approaching the quantum limit of diffusion for a particle of mass m. Conversely, the spin drag rate reaches a maximum value of $\Gamma_{sd} \simeq 1.2 k_B T_F/\hbar$ in terms of the Fermi temperature T_F. The frequency-dependent spin conductivity $\sigma_s(\omega)$ exhibits a broad Drude peak, with spectral weight transferred to a universal high-frequency tail $\sigma_s(\omega \to \infty) = \hbar^{1/2}C/3\pi(m\omega)^{3/2}$ proportional to the Tan contact density C. For the spin susceptibility $\chi_s(T)$ we find no downturn in the normal phase.

The excitation and decay of spin currents plays an important role in many areas of condensed matter physics, including the development of electronic devices based on spin transport. While the Coulomb interaction does not affect electrical currents in a uniform system [1], it transfers momentum between spin-up and down particles and thereby dampens the spin current. Understanding the mechanism of spin drag and spin diffusion quantitatively is important for an effective control of spin currents; however, in solids this is often complicated by the presence of impurities and lattice effects. Ultracold atomic Fermi gases provide an extremely clean experimental realization to study the effect of the two-particle interaction alone [2]. If the interactions are short-ranged and the scattering length is much larger than the particle spacing the results are universal and apply to a wide range of models, including dilute nuclear matter.

The spin diffusivity D_s measures how quickly a spin current levels out a gradient in the spin density. In a strongly interacting Fermi gas D_s decreases as the temperature is lowered into the quantum degenerate regime and reaches a minimum near the Fermi temperature T_F, before increasing again at even lower temperatures in the superfluid phase. The minimum value of D_s in the strong-coupling region can be understood qualitatively as a consequence of the uncertainty principle: the mean-free path in a gas cannot become shorter than the mean particle spacing in the absence of localization [3], which translates into a quantum bound $D_s \gtrsim \hbar/m$ for particles of mass m. For a strongly interacting Fermi gas of trapped ⁶Li atoms a spin diffusivity $D_s \geq 6.3(3)\hbar/m$ has recently been measured [4]. Very low spin diffusion is found also in graphene [5], while spin Coulomb drag in GaAs quantum wells yields a value of $D_s \gtrsim 500\hbar/m$ [6].

The determination of D_s near its minimum in the strongly interacting regime, and more generally the question of whether quantum mechanics imposes universal lower bounds on the transport coefficients, is a key challenge in many-body physics. Recent progress comes from the anti–de Sitter and conformal field theory correspondence which maps a strongly coupled field theory to an equivalent weakly coupled gravitational theory, where calculations are feasible. It gives a lower quantum bound for the internal friction of mass flow, expressed as the ratio of shear viscosity to entropy $\eta/s \geq \hbar/4\pi k_B$, in certain relativistic field theories [7]. Quantum limited friction, or perfect fluidity [8], has been found to be almost satisfied in very different physical situations ranging from quark-gluon plasmas to ultracold atomic gases [9–11]. It remains an open question whether a similar bound exists for spin diffusion in nonrelativistic systems [12].

In this work we present a strong-coupling calculation of the spin diffusivity D_s in the unitary Fermi gas. At infinite scattering length it saturates the unitarity bound on the scattering cross section and is one of the most strongly interacting systems known; it is also the only known example of a nonrelativistic interacting scale-invariant fluid. The unitary gas becomes superfluid below the transition temperature $T_c \simeq 0.16 T_F$ [13]; here we focus on the normal phase above T_c where transport experiments are available and where the most interesting features occur. In Fig. 1 our result for the diffusivity is shown by the solid red line, and we find a minimum value of $D_s \simeq 1.3\hbar/m$ at a temperature of about $T = 0.5 T_F$. To our knowledge this is the lowest value achieved to date for a strong two-particle interaction. Recent experimental data for the trapped unitary gas [4] are shown as the blue squares (see caption), and we obtain remarkable agreement for all temperatures in the normal phase.

In the high-temperature limit where $D_s \gg \hbar/m$ is much larger than the quantum limit our calculation agrees with the predictions of Boltzmann kinetic theory [4,14–16]
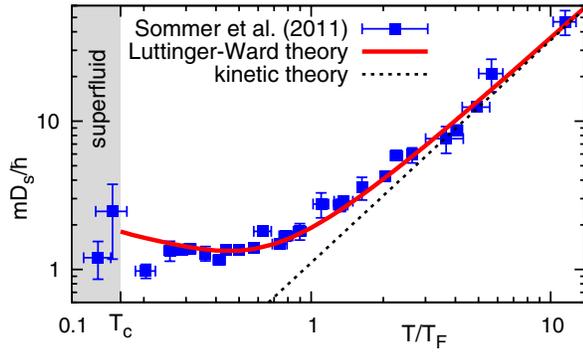
FIG. 1 (color online).   Spin diffusivity D_s vs reduced temperature T/T_F (solid red line) in the normal phase, $T > T_c \simeq 0.16 T_F$. The experimental data [4] (blue squares) for the trapped gas are rescaled down by a factor of 4.7 to compensate for the effect of the trapping potential. The dashed black line is the result from kinetic theory, $D_s = 1.1(T/T_F)^{3/2}\hbar/m$.

(dashed black line). In the strongly interacting region near T_c, however, the fermions cease to be well-defined quasiparticles [17,18] and the Boltzmann theory is not applicable. Therefore, we employ the strong coupling Luttinger-Ward theory to compute spin transport. The Luttinger-Ward (or 2PI) formalism [19,20] is based on the self-consistent T matrix for repeated particle-particle scattering and becomes exact at high temperatures. In the most interesting regime near T_c and unitarity there is no small parameter to estimate its accuracy. Instead, a comparison with experiment shows that it accurately describes both the normal and the superfluid phase of the BEC-BCS crossover problem [21]: the values for $T_c/T_F = 0.16(1)$ and the Bertsch parameter $\xi = 0.36(1)$ agree within error bounds with precision experimental [13] and diagrammatic Monte Carlo [22] results. We have devised a framework which includes all diagrams needed to exactly fulfill the conservation laws including scale invariance [9] and the Tan relations [11].

The Luttinger-Ward theory has recently been extended to compute transport coefficients in linear response using the Kubo formula: this gives access to the frequency-dependent shear viscosity of the unitary Fermi gas, which was found to satisfy the exact viscosity sum rule [9,23]. We now extend this work to the case of spin transport in order to explain the recent experiment by Sommer *et al.* [4], and we proceed as follows: first we compute the frequency-dependent spin conductivity $\sigma_s(\omega)$ of the unitary Fermi gas. The dc value $\sigma_s = \sigma_s(\omega = 0)$ determines the spin drag rate $\Gamma_{sd} = n/m\sigma_s$ at density n, which is the rate of momentum transfer between atoms of opposite spin. We then compute the spin susceptibility $\chi_s = \partial(n_\uparrow - n_\downarrow)/\partial(\mu_\uparrow - \mu_\downarrow)$ which characterizes the magnetic properties of the system [14,24]. Finally, we determine the spin diffusivity shown in Fig. 1 by the Einstein relation $D_s = \sigma_s/\chi_s$.

The strongly interacting two-component Fermi gas is described by the grand canonical Hamiltonian

$$\mathcal{H} = \sum_{\boldsymbol{k},\sigma}(\varepsilon_{\boldsymbol{k}} - \mu_\sigma)c^\dagger_{\boldsymbol{k}\sigma}c_{\boldsymbol{k}\sigma} + \frac{g_0}{V}\sum_{\boldsymbol{k},\boldsymbol{k}',\boldsymbol{q}} c^\dagger_{\boldsymbol{k}\uparrow}c^\dagger_{\boldsymbol{k}'\downarrow}c_{\boldsymbol{k}'-\boldsymbol{q}\downarrow}c_{\boldsymbol{k}+\boldsymbol{q}\uparrow}$$

where $\varepsilon_{\boldsymbol{k}} = k^2/2m$ ($\hbar \equiv 1$) is the free particle dispersion and μ_σ the chemical potential for the $\sigma = \uparrow, \downarrow$ components. The s-wave contact interaction g_0 acts only between different fermion species at low temperatures. The bare interaction is singular in the ultraviolet [2] and needs to be regularized; the renormalized coupling $g = 4\pi\hbar^2 a/m$ determines the s-wave scattering length a.

The transport coefficients are obtained from the microscopic model via the retarded number-current or spin-current correlation function

$$\chi_{\text{jn/js}}(\boldsymbol{q}, \omega) = \frac{i}{\hbar}\int_0^\infty dt \int d^3x\, e^{i(\omega t - \boldsymbol{q}\cdot\boldsymbol{x})}$$
$$\times \langle[(j_\uparrow^z \pm j_\downarrow^z)(\boldsymbol{x}, t), (j_\uparrow^z \pm j_\downarrow^z)(\boldsymbol{0}, 0)]\rangle. \quad (1)$$

The spin selective current operators in Fourier representation are given by $\boldsymbol{j}_\sigma(\boldsymbol{q}) = V^{-1}\sum_{\boldsymbol{k}}(\hbar\boldsymbol{k}/m)c^\dagger_{\boldsymbol{k}-\boldsymbol{q}/2,\sigma}c_{\boldsymbol{k}+\boldsymbol{q}/2,\sigma}$. The correlation function determines the conductivity

$$\sigma_{n/s}(\omega) = \lim_{q\to 0}\frac{\text{Im}\chi_{\text{jn/js}}(\boldsymbol{q}, \omega)}{\omega} \quad (2)$$

which measures the relaxation of a global number or spin current at frequency ω. The total response integrated over all frequencies is proportional to the particle density by the number or spin f-sum rule [25,26]

$$\int_{-\infty}^\infty \frac{d\omega}{\pi}\sigma_{n/s}(\omega) = \frac{n}{m}. \quad (3)$$

For a momentum-conserving interaction the particle current cannot decay and $\sigma_n(\omega) = \pi n\delta(\omega)/m$. In contrast, scattering transfers momentum between $\uparrow$ and $\downarrow$ particles so that the spin current relaxes and $\sigma_s(\omega)$ has a nontrivial structure.

We compute the current correlation function (1) using field theoretical methods and Feynman diagrams in the Matsubara formalism [25]. The current operator $j^z = j_\uparrow^z \pm j_\downarrow^z$ implies a current response vertex $J_{\sigma\sigma'} = J_{\sigma\sigma'}^0 + J_{\sigma\sigma'}^{\text{MT}} + J_{\sigma\sigma'}^{\text{AL}}$ in the Feynman diagrams which splits into three contributions [9,20] (σ, σ' are the spin indices of incoming and outgoing fermion lines). The first term is the bare number (spin) current vertex $J_{\sigma\sigma'n}^0(\boldsymbol{p}) = p_z\tau_{\sigma\sigma'}^0$ [$J_{\sigma\sigma's}^0(\boldsymbol{p}) = p_z\tau_{\sigma\sigma'}^3$] with the $\ell = 1$ partial wave component of the momentum $\boldsymbol{p}$ and Pauli matrices τ^j. The other two terms are current vertex corrections which are required to fulfill the conservation laws. The Maki-Thompson (MT) contribution describes direct scattering between quasiparticles while the Aslamazov-Larkin (AL) term captures the induced current of fermion pairs, or molecules (for details see Ref. [9]). For a mass current both $\uparrow$ and $\downarrow$ fermions move in the same direction and induce a current of pairs, leading to a sizeable AL term. In contrast, for a spin current $\uparrow$ and $\downarrow$ atoms move in opposite directions [4] and no pair current is

induced. Hence, the Aslamazov-Larkin correction to the spin current vanishes exactly in the spin balanced case, $J_{\sigma\sigma's}^{AL} = 0$, which constitutes an important simplification.

We solve the self-consistent equation for the fully dressed current vertex $J_{\sigma\sigma'}$ by iteration and obtain the current correlation function (1) via the Kubo formula [9]. Since the correlation function $\chi_{jn/js}(q = 0, i\omega_m)$ is evaluated at discrete imaginary Matsubara frequencies $i\omega_m$, we must perform an analytic continuation in order to obtain the physically relevant correlation function $\chi_{jn/js}(\omega)$ for real frequencies ω. We use Padé approximants and find that the continuation is robust at low temperatures if we vary the number of Matsubara frequencies, and it yields the correct high-frequency tail (see below). Specifically, we oversample the Matsubara data twice with a spline fit and use the first five Matsubara frequencies in order to extract the spin drag rate Γ_{sd}. We validate our strong coupling calculation by confirming that $\sigma_s(\omega)$ indeed fulfills the spin f-sum rule (3) within 1%. Since we have constructed the formalism to satisfy the sum rules exactly, this quantifies the numerical accuracy of our self-consistent solution and the analytical continuation.

Spin conductivity.—The resulting spin conductivity $\sigma_s(\omega)$ is shown in Fig. 2 for reduced temperature $T/T_F = 0.5$ where it has the lowest dc value $\sigma_s = 0.8n/m$ (red circles). In a Drude model the conductivity would assume a form $\sigma_s^{Drude}(\omega) = (n/m)\Gamma_{sd}/(\omega^2 + \Gamma_{sd}^2)$ (solid black line) with total spectral weight given by the sum rule. The spin drag rate Γ_{sd} is a parameter which we determine from the dc limit $\sigma_s = n/m\Gamma_{sd}$ of our full numerical solution. We find that the true $\sigma_s(\omega)$ deviates from the Drude model for $\omega \gtrsim E_F$: spectral weight is transferred from the region $\omega \lesssim 8E_F$ to higher frequencies where it forms a power-law tail $\sigma_s(\omega \to \infty) \sim \omega^{-3/2}$ (dotted blue line in Fig. 2).

The high-frequency response generally depends on the nonuniversal short-distance behavior of the interatomic potential. However, for a broad Feshbach resonance as in
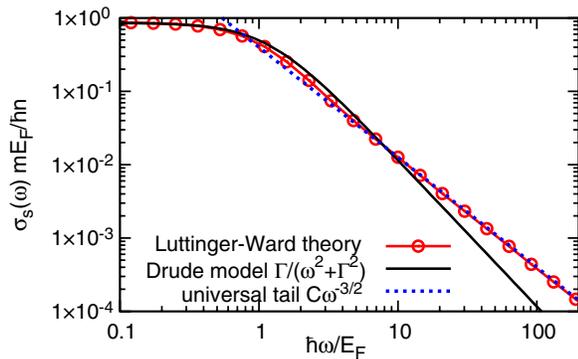
^{6}Li [2] this potential has a range much shorter than the particle spacing, $k_F|r_e| \ll 1$, and becomes effectively a contact interaction. In this case the correlation functions exhibit universal power-law tails in the high-frequency range $\max(E_F, k_BT)/\hbar \ll \omega \ll \hbar/(mr_e^2)$ [27] which depend only on the Tan contact density C [28]. In the high-frequency limit the exact transport equations can be solved analytically in a manner analogous to the viscosity response [9], and we obtain the universal spin conductivity tail

$$\sigma_s(\omega \to \infty) = \frac{\hbar^{1/2}C}{3\pi(m\omega)^{3/2}} \qquad (4)$$

in agreement with the result from the operator product expansion [29]. Similar tails appear in other transport properties such as the viscosity [9,23,29,30]. The value for the Tan contact density $C = 0.0863k_F^4$ at $T/T_F = 0.5$ extracted from the tail of $\sigma_s(\omega)$ agrees better than 1% with the value $C = 0.0860k_F^4$ from the tail of the momentum distribution $n_k \sim Ck^{-4}$ [9]. A similar behavior of $\sigma_s(\omega)$ is observed for all temperatures $T \geq T_c$.

We now turn to the dc limit and plot the spin drag rate $\Gamma_{sd} = n/m\sigma_s$ in Fig. 3 (solid red line). The spin drag has a maximum value of $\Gamma_{sd} \approx 1.2E_F/\hbar$ in the quantum degenerate regime around $T/T_F = 0.5$ and decreases both for lower and higher temperatures. In the high-temperature limit of a classical gas the Luttinger-Ward transport equations can be solved analytically to leading order in the fugacity [9], and we obtain $\Gamma_{sd} = (32\sqrt{2}/9\pi^{3/2}) \times (T/T_F)^{-1/2}E_F/\hbar = 0.9(T/T_F)^{-1/2}E_F/\hbar$ for $T \gg T_F$ in agreement with Boltzmann kinetic theory [4,15]. The fact that the numerical solution at large temperatures agrees with the analytical result for $T \gg T_F$ is a nontrivial validation of our analytical continuation procedure.

The measured spin drag rate in a trapped unitary Fermi gas [4] (blue squares in Fig. 3) has the same qualitative behavior as our numerical data, with a broad maximum between $T/T_F = 0.4, \ldots, 0.8$. Note that the absolute spin drag rate cannot be directly compared to our calculation for
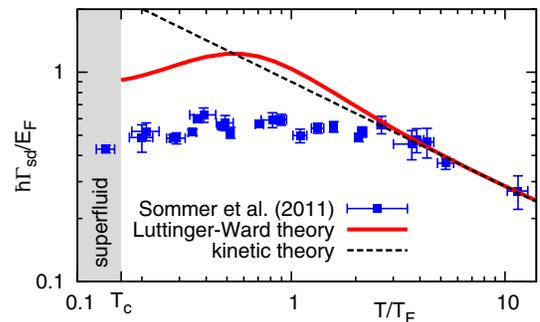

FIG. 2 (color online). Spin conductivity $\sigma_s(\omega)$ (in units of $\hbar n/mE_F$) vs frequency (red circles) at $T = 0.5T_F$. The Drude model (solid black line) has the same total spectral weight as $\sigma_s(\omega)$ given by the spin f-sum rule. Part of the spectral weight is transferred from lower frequencies into a universal high-frequency tail (dotted blue line) $\sigma_s(\omega \to \infty) = C/3\pi(m\omega)^{3/2}$ with Tan contact density $C = 0.086k_F^4$ [9].

FIG. 3 (color online). Spin drag rate Γ_{sd} (in units of $E_F/\hbar$) vs reduced temperature T/T_F (solid red line). The experimental data [4] (blue squares) for a trapped gas are rescaled up by a factor of 5.3 to compensate for the effect of the trapping potential. The dashed black line is the result from kinetic theory, $\Gamma_{sd} = 0.9(T/T_F)^{-1/2}E_F/\hbar$.

the uniform system: the solution of the transport equation depends on the trap geometry and the velocity profiles of $\uparrow$ and $\downarrow$ particles in the trap [4,16,31]. For a quadratic velocity profile in a harmonic trap the spin drag rate $\Gamma_{\mathrm{sd}}^{\mathrm{trap}} = \Gamma_{\mathrm{sd}}/\alpha$ is rescaled by a constant factor $\alpha = 2^{5/2}$ in the high-temperature limit (see supplementary information of Ref. [4]). In the experiment a factor of $\alpha = 5.6(4)$ is found, and we obtain the best fit at high temperatures for $\alpha = 5.3$. In the quantum degenerate regime $T \lesssim T_F$ the assumption of a uniform quadratic velocity profile breaks down: in the center of the trap a large spin drag leads to slow spin motion, while the spins in the weakly interacting wings move rapidly. The velocity profile thus becomes nonuniform and α acquires a temperature dependence. In Fig. 3 the calculation for the uniform system and the rescaled trap-averaged data differ for $T \lesssim T_F$, and the scaling factor starts to deviate from the high-T estimate $\alpha = 5.3$.

Spin susceptibility.—We shall compute and discuss the spin susceptibility χ_s in order to find $D_s = \sigma_s/\chi_s$. Both the spin susceptibility $\chi_s = \partial(n_\uparrow - n_\downarrow)/\partial(\mu_\uparrow - \mu_\downarrow)$ and the normalized compressibility $\chi_n = n^2\kappa = \partial(n_\uparrow + n_\downarrow)/\partial(\mu_\uparrow + \mu_\downarrow)$ are obtained from the number or spin correlation function

$$\chi_{n/s} = \frac{i}{\hbar} \int_0^\infty dt\, d^3x \langle [(n_\uparrow \pm n_\downarrow)(\boldsymbol{x}, t), (n_\uparrow \pm n_\downarrow)(\boldsymbol{0}, 0)] \rangle.$$

The spin-selective particle number operator in Fourier representation reads $n_\sigma(\boldsymbol{q}) = V^{-1}\sum_k c_{\boldsymbol{k}-\boldsymbol{q}/2,\sigma}^\dagger c_{\boldsymbol{k}+\boldsymbol{q}/2,\sigma}$. In the Luttinger-Ward formulation the bare number (spin) density vertex has the form $N_{\sigma\sigma' n}^0 = \tau_{\sigma\sigma'}^0$ ($N_{\sigma\sigma' s}^0 = \tau_{\sigma\sigma'}^3$). For the dressed number density vertex N_n both MT and AL vertex corrections contribute, while the AL term again vanishes for N_s in the spin balanced case. In order to obtain the static susceptibility $\chi_{n/s}$ we calculate the susceptibility $\chi_{n/s}(i\omega_m = 0)$ for zero Matsubara frequency; note that an analytical continuation is not needed here. The static limit of the related *current* correlation function $\chi_{\mathrm{jn/js}} = \chi_{\mathrm{jn/js}}(i\omega_m = 0) = n/m$ is fixed by the exact f-sum rule (3), and our numerical computation fulfills this sum rule within 1% (see above). We therefore expect our results for the static susceptibilities $\chi_{n/s}$ to be of the same accuracy.

The susceptibility of the free Fermi gas is $\chi_{n,s}^0 = n/k_B T$ for $T \gg T_F$ (Curie-Weiss) and $\chi_{n,s}^0 = \chi_0 = 3n/2E_F$ for $T \to 0$ in the Fermi liquid phase (dashed black line in Fig. 4). In the unitary Fermi gas the attractive interaction leads to a compressiblity χ_n twice as large as χ_n^0 in the quantum degenerate regime near T_c (open magenta circles), in very good agreement with the experimental data [4] (full cyan circles) and with a non-self-consistent diagrammatic approach [32]. Conversely, we find that the spin susceptibility χ_s remains below χ_s^0 and exhibits a maximum of about $\chi_s \simeq 0.4\chi_0$ at $T/T_F = 0.3$ (open red squares). The spin susceptibility is expected to vanish as
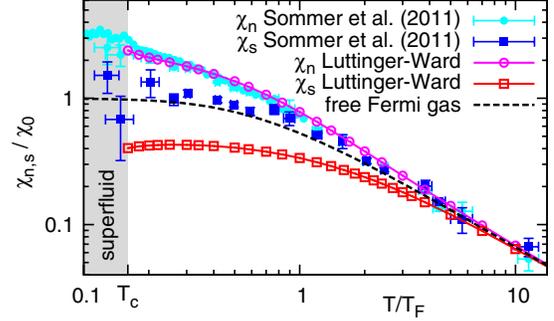

FIG. 4 (color online). Compressibility χ_n (circles) and spin susceptibility χ_s (squares) vs reduced temperature T/T_F. The experimental data [4] (full symbols) are compared to our Luttinger-Ward calculation (open symbols). The dashed black line is the susceptibility of the free Fermi gas.

$\exp(-2\Delta/k_B T)$ deep in the superfluid phase with gap Δ, where an infinitesimal magnetic field gradient cannot break pairs. The proposed pseudogap scenario [18,32] predicts a pronounced drop of χ_s at a pair-breaking scale $T^* > T_c$. Our data, which fully include the attractive branch, remain nearly constant down to $T/T_F \simeq 0.2$. This indicates that the scales T^* and T_c are very close in the unitary Fermi gas. The measured χ_s (full blue squares in Fig. 4) also shows no downturn and can be described in a Fermi liquid picture despite the large value for $T_c/T_F \simeq 0.16$, in agreement with a recent quantum Monte Carlo and experimental study [33]. Note that a finite condensate fraction can lead to significantly lower values for χ_s [34].

In the experiment by Sommer *et al.* [4] χ_s is determined from a combination of the local spin density gradient and the trap-averaged center of mass motion. Hence, the measured χ_s deviates at low temperatures from the calculation of the uniform system (cf. Fig. 4) for similar reasons as discussed above for Γ_{sd}. Remarkably, we find that the differences in Γ_{sd} and χ_s cancel and lead to a very good agreement in the spin diffusivity $D_s = n/m\Gamma_{\mathrm{sd}}\chi_s$ shown in Fig. 1 above.

In conclusion, our strong coupling calculation of spin transport explains the behavior of the spin diffusivity D_s seen in experiment [4], and we find that the diffusivity of the unitary Fermi gas reaches the quantum limit $\hbar/m$. This provides an important constraint for any future spin transport bound from gravity duals [12]. We predict a universal high-frequency tail of the spin conductivity $\sigma_s(\omega)$ which should be accessible experimentally using Bragg spectroscopy for the dynamic structure factor [35]. It would be desirable to have local measurements of transport properties in a way similar to local precision measurements of the thermodynamic properties [13] and the momentum distribution [36].

[1] J. M. Ziman, *Electrons and Phonons* (Oxford University Press, Oxford, 1960).

[2] I. Bloch, J. Dalibard, and W. Zwerger, Rev. Mod. Phys. **80,** 885 (2008).

[3] S. Sachdev, *Quantum Phase Transitions* (Cambridge University Press, Cambridge, England, 1999).

[4] A. Sommer, M. Ku, G. Roati, and M. W. Zwierlein, Nature (London) **472,** 201 (2011); A. Sommer, M. Ku, and M. W. Zwierlein, New J. Phys. **13,** 055009 (2011).

[5] M. Müller and H. C. Nguyen, New J. Phys. **13,** 035009 (2011).

[6] C. P. Weber, N. Gedik, J. E. Moore, J. Orenstein, J. Stephens, and D. D. Awschalom, Nature (London) **437,** 1330 (2005).

[7] G. Policastro, D. T. Son, and A. O. Starinets, Phys. Rev. Lett. **87,** 081601 (2001); P. K. Kovtun, D. T. Son, and A. O. Starinets, Phys. Rev. Lett. **94,** 111601 (2005).

[8] T. Schäfer and D. Teaney, Rep. Prog. Phys. **72,** 126001 (2009); A. Adams, L. D. Carr, T. Schäfer, P. Steinberg, and J. E. Thomas, arXiv:1205.5180.

[9] T. Enss, R. Haussmann, and W. Zwerger, Ann. Phys. (N.Y.) **326,** 770 (2011).

[10] C. Cao, E. Elliott, J. Joseph, H. Wu, J. Petricka, T. Schäfer, and J. E. Thomas, Science **331,** 58 (2011); G. Wlazłowski, P. Magierski, and J. E. Drut, Phys. Rev. Lett. **109,** 020406 (2012); T. Enss, C. Küppersbusch, and L. Fritz, Phys. Rev. A **86,** 013617 (2012); A. Kryjevski, arXiv:1206.0059.

[11] T. Enss, Phys. Rev. A **86,** 013616 (2012).

[12] D. T. Son, Phys. Rev. D **78,** 046003 (2008); P. Kovtun and A. Ritz, Phys. Rev. D **78,** 066009 (2008).

[13] M. J. H. Ku, A. T. Sommer, L. W. Cheuk, and M. W. Zwierlein, Science **335,** 563 (2012).

[14] R. A. Duine, M. Polini, H. T. C. Stoof, and G. Vignale, Phys. Rev. Lett. **104,** 220403 (2010).

[15] G. M. Bruun, New J. Phys. **13,** 035005 (2011).

[16] G. M. Bruun and C. J. Pethick, Phys. Rev. Lett. **107,** 255302 (2011).

[17] R. Haussmann, M. Punk, and W. Zwerger, Phys. Rev. A **80,** 063612 (2009).

[18] J. P. Gaebler, J. T. Stewart, T. E. Drake, D. S. Jin, A. Perali, P. Pieri, and G. C. Strinati, Nat. Phys. **6,** 569 (2010);

D. Wulin, H. Guo, C.-C. Chien, and K. Levin, Phys. Rev. A **83,** 061601(R) (2011).

[19] J. M. Luttinger and J. Ward, Phys. Rev. **118,** 1417 (1960).

[20] G. Baym and L. P. Kadanoff, Phys. Rev. **124,** 287 (1961).

[21] R. Haussmann, Z. Phys. B **91,** 291 (1993); R. Haussmann, Phys. Rev. B **49,** 12975 (1994); R. Haussmann, W. Rantner, S. Cerrito, and W. Zwerger, Phys. Rev. A **75,** 023610 (2007).

[22] K. Van Houcke, F. Werner, E. Kozik, N. Prokof'ev, B. Svistunov, M. J. H. Ku, A. T. Sommer, L. W. Cheuk, A. Schirotzek, and M. W. Zwierlein, Nat. Phys. **8,** 366 (2012).

[23] E. Taylor and M. Randeria, Phys. Rev. A **81,** 053610 (2010).

[24] S. Stringari, Phys. Rev. Lett. **102,** 110406 (2009).

[25] A. A. Abrikosov, L. P. Gorkov, and I. E. Dzyaloshinski, *Methods of Quantum Field Theory in Statistical Physics* (Dover, New York, 1975).

[26] T. Enss, arXiv:1209.3317.

[27] E. Braaten, in *The BCS-BEC Crossover and the Unitary Fermi Gas*, edited by W. Zwerger (Springer, Berlin, 2012), p. 193.

[28] S. Tan, Ann. Phys. (N.Y.) **323,** 2971 (2008).

[29] J. Hofmann, Phys. Rev. A **84,** 043603 (2011).

[30] W. D. Goldberger and Z. U. Khandker, Phys. Rev. A **85,** 013624 (2012); E. Taylor and M. Randeria, Phys. Rev. Lett. **109,** 135301 (2012).

[31] O. Goulko, F. Chevy, and C. Lobo, Phys. Rev. A **84,** 051605 (2011); O. Goulko, F. Chevy, and C. Lobo, New J. Phys. **14,** 073036 (2012).

[32] F. Palestini, P. Pieri, and G. C. Strinati, Phys. Rev. Lett. **108,** 080401 (2012).

[33] S. Nascimbène, N. Navon, S. Pilati, F. Chevy, S. Giorgini, A. Georges, and C. Salomon, Phys. Rev. Lett. **106,** 215303 (2011).

[34] C. Sanner, E. J. Su, A. Keshet, W. Huang, J. Gillen, R. Gommers, and W. Ketterle, Phys. Rev. Lett. **106,** 010402 (2011).

[35] S. Hoinka, M. Lingham, M. Delehaye, and C. J. Vale, Phys. Rev. Lett. **109,** 050403 (2012).

[36] T. E. Drake, Y. Sagi, R. Paudel, J. T. Stewart, J. P. Gaebler, and D. S. Jin, Phys. Rev. A **86,** 031601 (2012).